Calculations in the Liquid-Drop Model of Fission

S. FRANKEL* AND N. METROPOLIS
Institute for Nuclear Studies, University of Chicago, Chicago, Illinois
(Received May 6, 1947)

The liquid-drop model of fission as developed by Bohr and Wheeler and others has been studied with the use of an electronic calculator, the Eniac. Classical deformation energies have been calculated for many shapes not all near-spherical. The shapes considered were axially and primarily, but not exclusively, bilaterally symmetric, and single-valued in polar representation. Previous calculations are confirmed and extended. Agreement with observed fission thresholds and spontaneous fission rates is obtained. No explanation of asymmetric fission is found.

1. INTRODUCTION

IT has been recognized since the discovery of fission that this phenomenon permits a classical interpretation in terms of the liquid-drop model of the nucleus. It was pointed out by Meitner and Frisch[1] that the stability of the spherical shape of the liquid-drop model nucleus, owing to the surface tension characteristics of the short range nuclear forces, is, to a large extent, counteracted for very heavy nuclei by the Coulomb repulsion. Shortly thereafter a more detailed study of the effects of these opposing influences was made by Bohr and Wheeler[2] and independently by Frenkel.[3] They showed that a uniformly charged droplet is unstable with respect to deformation at constant volume into a prolate spheroid if the ratio of the Coulomb energy to surface tension energy exceeds 2. Following Bohr and Wheeler, this ratio is here denoted by $2x$.

For lesser values of this ratio the spherical shape is stable with respect to any small deformation. However, for any value of this ratio greater than 0.70, i.e., for $x>0.35$, the potential energy (surface plus Coulomb) is diminished by separating the drop into two equal spheres far removed from each other. Thus for x between 0.35 and 1.0 (true for all heavy nuclei) the initial spherical configuration is a relative (local) minimum of the potential energy but not an absolute minimum. If the nucleus is continuously deformed from its initial spherical configuration to this two-droplet final configuration the potential energy first rises, say by an amount ΔE, then falls to less than its initial value. The least of these values, ΔE, considering all possible deformation trajectories, is the reaction threshold and the deformation at which it occurs must be a saddle-point of the potential energy.

The reaction threshold can be calculated for nuclei close to the stability limit, i.e., x close to unity, by the following method.[2–5] The deformation is assumed axially symmetric and expressed as a series in Legendre polynomials. The potential energy is then expanded as a power series in the coefficients of this expression. By evaluating a few terms in this power series the potential energy can be found for small deformations. If x is sufficiently close to unity the saddle-point occurs within this range of deformations and its position and potential energy can be determined.

Bohr and Wheeler[2] used this method to determine the first two terms in the expansion of ΔE as a function of $(1-x)$. This required calculating terms up to the fourth power of the P_2 component of the deformation and the square of the P_4 component.

Present and Knipp[4] extended this series somewhat and introduced also odd terms, P_3 and P_5. F. Reines, working with Present and Knipp, included additional terms to an extent sufficient to permit the determination of the saddle-point shape and the reaction threshold in the range $1.0 \geqslant x \geqslant 0.8$.[5] The value and derivative

* Now with Frankel and Nelson, Los Angeles.
[1] L. Meitner and O. R. Frisch, Nature **143**, 239 (1939).
[2] N. Bohr and J. Wheeler, Phys. Rev. **56**, 426 (1939).
[3] J. Frenkel, Phys. Rev. **55**, 987 (1939) and J. Phys. U.S.S.R. **1**, 125 (1939).
[4] R. D. Present and J. K. Knipp, Phys. Rev. **57**, 751, 1188 (1940).
[5] R. D. Present, F. Reines, and J. K. Knipp, Phys. Rev. **70**, 557 (1946).

of the threshold at $x=0$ have been given by Bohr and Wheeler.[2] Using these values and his results Reines determined by interpolation the value of the threshold for $x=0.74$ (corresponding to U^{239}). His estimated limit of error is ± 15 percent.

During the last stages of the development of the Eniac (the "electronic numerical integrater and computer") Professor Fermi suggested to the authors that the use of the Eniac might permit a straightforward numerical calculation of the potential energy values beyond the range of validity of the power series.

2. THEORY

The potential energy of a deformed nucleus in the liquid-drop model is the sum of two terms

$$E=E_s+E_c, \tag{1}$$

where E_s is a surface-tension-like energy arising from the lack of saturation of the binding forces of particles near the surface, and is proportional to the surface, while E_c is the Coulomb energy of the charge of the nucleus which is assumed uniformly distributed throughout its volume. The energy of the undeformed (spherical) nucleus is denoted by

$$E^0=E_s^0+E_c^0=E_s^0(1+2x). \tag{2}$$

Only axially symmetric distortions are considered. These are specified by giving the radius, R^1, as a function of the cosine of the co-latitude, μ. The unit of length is the undistorted radius. It is convenient to introduce a scale factor, R_0, and write

$$\begin{aligned} R^1(\mu)&=R_0R(\mu),\\ R(\mu)&=1+\alpha_1P_1(\mu)+\alpha_2P_2(\mu)+\cdots, \end{aligned} \tag{3}$$

where P_i is the ith Legendre polynomial. A particular distortion is specified by the coefficients α_i of this expansion. Only terms up to P_{10} have been considered.

It may be observed that (3) does not represent all axially symmetric deformations but only those described by single-valued functions, $R^1(\mu)$. Thus a deformation into two almost spherical parts connected by a thin filament cannot be so represented.

The scale factor R_0 is determined by the constant volume condition,

$$\tfrac{1}{2}\int_{-1}^{1}(R^1)^3d\mu=R_0^3V=1,$$

$$V=\tfrac{1}{2}\int_{-1}^{1}R^3(\mu)d\mu.$$

The energies, E_s and E_c, are represented in terms of their original values,

$$E_s=B_sE_s^0,\quad E_c=B_cE_c^0=2xB_cE_s^0. \tag{5}$$

The relative surface energy, B_s, is the ratio of the distorted to the undistorted surface.

$$B_s=\tfrac{1}{2}V^{-2/3}\int_{-1}^{1}R[R^2+\nu^2(dR/d\mu)^2]^{\frac{1}{2}}d\mu, \tag{6}$$

where

$$\nu^2=1-\mu^2.$$

B_c is similarly calculated for the volume bounded by $R(\mu)$, then normalized by multiplication by $V^{-5/3}$.

$$B_c=(15/16\pi^2)\left[V^{-5/3}\int\phi d\tau\right], \tag{7}$$

$$\phi=\int\frac{d\tau'}{|r-r'|}=\int_{-1}^{1}d\mu'\times\int_0^{R'(\mu')}r'^2dr'\int_0^{2\pi}\frac{d\psi'}{|r-r'|}. \tag{8}$$

The calculation of B_c thus involves calculating a sixfold integral, threefold in $d\tau'$ and threefold in $d\tau$. Since the shape is axially symmetric the azimuthal integration of $d\tau$ is trivial. B_c can be reduced further, to a fourfold integral, by the following device:[6] Consider another distorted drop having the same shape and charge density but scaled up in all linear dimensions by a factor $(1+\epsilon)$ where $\epsilon\ll 1$. Then the volume of the

TABLE I. Threshold values and saddle-point shapes.

x	ξ	B_s	B_c	α_2	α_4	α_6	α_8	α_{10}
0.9	0.0007	0.0195	0.0107	0.23	0.019	−0.0016	—	—
0.81	0.0050	0.0731	0.0420	0.47	0.083	−0.006	−0.006	—
0.77	0.009_3	0.094_2	0.055_1	0.5_5	0.1_1	−0.01	−0.01	—
0.74	0.0136	0.1371	0.0834	0.70	0.193	−0.008	−0.020	−0.0025
0.65	0.0400	0.3044	0.2034	2.4	1.15	−0.11	−0.22	0.03

[6] This method was suggested to us by Dr. H. Hurwitz.

second drop, hence also its charge, is greater than that of the first by a factor $(1+3\epsilon)$ and its electrostatic energy is greater by a factor $(1+5\epsilon)$. This second drop may be produced from the first by adding a thin layer of the (charged) material to its surface. The increase of electrostatic energy in this process is the work required to bring the added surface charge from infinity and thus depends only on the potentials on the surface.

$$5\epsilon E_c = 5\epsilon \int \phi d\tau = \int \phi(R, \omega)(\epsilon R) R^2 d\omega. \quad (9)$$

Hence

$$B_c = (3/8\pi V^{5/3}) \int \phi_s R^3 d\mu, \quad (10)$$

where ϕ_s is the potential at the surface as given by (8).

The azimuthal integration in the evaluation of ϕ can be carried out analytically and results in an elliptic integral of the first kind.

$$\int_0^{2\pi} [R^2+r'^2-2Rr'(\mu\mu'+\nu\nu'\cos\psi')]^{-\frac{1}{2}} d\psi'$$

$$= \int_0^{2\pi} [A_0^2 \cos^2(\psi'/2)+G_0^2 \sin^2(\psi'/2)]^{-\frac{1}{2}} d\psi'$$

$$\equiv I(A_0, G_0), \quad (11)$$

where

$$A_0^2 = R^2+r'^2-2Rr'(\mu\mu'+\nu\nu'),$$

$$G_0^2 = R^2+r'^2-2Rr'(\mu\mu'-\nu\nu').$$

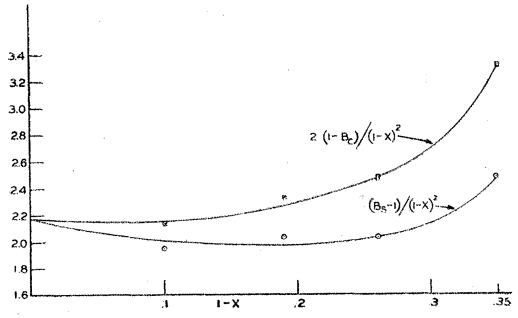

FIG. 2a. Dependence of the relative Coulomb energy, B_c, and the surface energy, B_s, of saddle-point shapes on x. (Cf. Eqs. (5)–(7)).

Landen's transformation,[7]

$$I(A_n, G_n) = I(A_{n+1}, G_{n+1}) \quad (12)$$

$$A_{n+1} = (A_n+G_n)/2, \quad G_{n+1} = (A_n G_n)^{\frac{1}{2}}$$

provides the basis of a convenient[8] iterative scheme for evaluating $I(A_0, G_0)$. On successive applications of this transformation the difference, $|A_n-G_n|$, rapidly approaches zero. Then denoting the common limit of A_n and G_n by M (the "arithmetic-geometric mean" of A_0 and G_0),

$$I(A_0 G_0) = 2\pi/M. \quad (13)$$

The number of steps in the iteration procedure was left free in the planning of the problem. Calculating experience showed that sufficient accuracy was obtained by carrying the calculation to A_4 (cf. Appendix II).

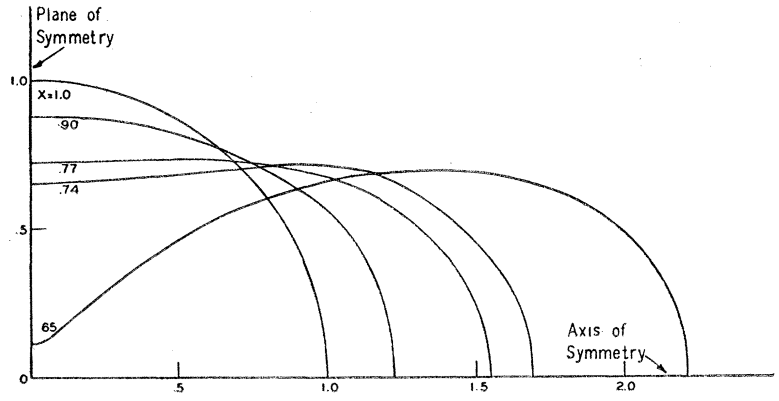

FIG. 1. Saddle-point shapes for various values of the nuclear parameter x. The unit of length is the undistorted radius.

[7] E. T. Whittaker and G. N. Watson, *Modern Analysis* (Cambridge University Press, Teddington, England, 1915), p. 533.

[8] In treating this problem with a desk calculator the use of a table of the first elliptic integral in this step would be far easier. However, in setting up the problem for the Eniac the economy in program controls and programming labor of this procedure seemed to us adequate compensation for the increase in computing time. It seems likely that the use of high speed calculating machines will often effect changes of this kind in the economy of calculating procedures.

The radial integration in the evaluation of ϕ and both co-latitude integrations were carried out numerically. In the radial integration the relative radius

$$y=r'/R'(\mu') \tag{14}$$

with the range (0, 1) was used as argument. A five-point integration rule was used,[9]

$$3\int_0^1 f(y)y^2dy\cong\sum_{i=1}^{5} e_i f(y_i), \tag{15}$$

$y_i=0.2,\ 0.4,\ 0.6,\ 0.8,\ 1.0,$

$e_i=0.014881,\ 0.148809,\ 0.089286,\ 0.565476,\ 0.181548.$

The coefficients are so chosen that the equality sign holds for any fourth-degree polynomial, $f_4(x)$.[10]

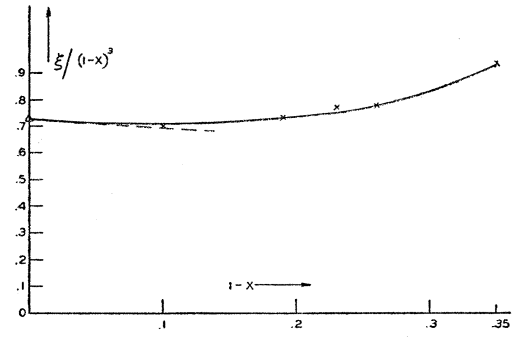

FIG. 2b. Relative threshold values. It is convenient to use $\xi/(1-x)^3$ as ordinate rather than ξ itself; cf. Eq. (23). The initial slope and intercept are taken from Bohr and Wheeler.

The co-latitude integrations in ϕ, B_c, B_s, and V are performed with a 10-entry gauss integration rule.[11] Denoting the ten roots of $P_{10}(\mu)$ by μ_i and the integration coefficients normalized to unity by c_i the equation

$$\tfrac{1}{2}\int_{-1}^{1} f(\mu)d\mu=\sum_{i=1}^{10} c_i f(\mu_i) \tag{16}$$

holds with the equality sign if $f(\mu)$ is a polynomial of 19th degree. Thus the various integrals are approximated by summations as follows:

$$V\cong\sum_{i=1}^{10} c_i R_i^3, \tag{17}$$

$$R_i=1+\sum_{j=1}^{10}\alpha_j P_j(\mu_i), \tag{18}$$

$$(dR/d\mu)_i=\sum_{j=1}^{10}\alpha_j P_j'(\mu_i),$$

$$B_s\cong V^{-2/3}\sum_{i=1}^{10} c_i R_i[R_i^2+\nu^2(dR/d\mu)_i^2]^{\frac{1}{2}}, \tag{19}$$

$$B_c\cong V^{-5/3}\sum_{i=1}^{10}\sum_{j=1}^{10}\sum_{k=1}^{5} c_i c_j e_k R_i^3 R_j^3/M_{ijk}, \tag{20}$$

$$2\pi/M_{ijk}=I(A_0, G_0), \tag{21}$$

$$A_0^2=R_i^2+R_j^2y_k^2-2R_iR_jy_k(\mu_i\mu_j+\nu_i\nu_j),$$

$$G_0^2=R_i^2+R_j^2y_k^2-2R_iR_jy_k(\mu_i\mu_j-\nu_i\nu_j).$$

The contributions to B_c for $k=5$ ($x_5=1.0$) require special treatment. The surface potential (say at R_j, μ_j) produced by a shell of material at the surface is represented by the integral

$$\int_{-1}^{1} d\mu'/M(\mu_j, \mu') \tag{22}$$

where $M(\mu_j, \mu')$ is the arithmetic-geometric average of the maximum and minimum distances from the point $(R_j, \mu_j, 0)$ to the circle (R', μ', ψ'). For $\mu'=\mu_i$, $i\neq j$, M has the value $M_{j,i,5}$ as defined in (21). However as μ' approaches μ_j the integrand, $1/M$, approaches infinity logarithmically. Thus the numerical approximation (16) is inapplicable to the integral (22). This difficulty is circumvented by separating the integrand, $1/M$, into a non-singular part which is integrated numerically in the usual way and a simple singular part which is integrated analytically. In the summation (20) each term, $1/M_{i,j,k}$, for which $i=j$, $k=5$ is replaced by the sum of two terms, one of which is the

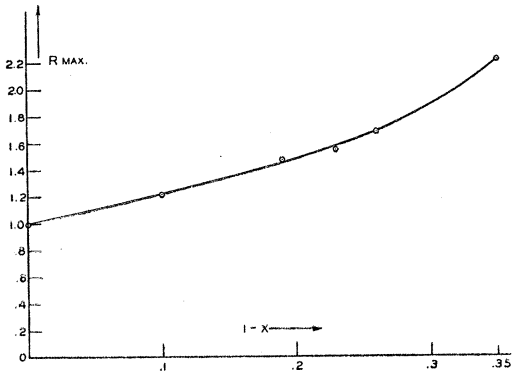

FIG. 2c. Maximum radii of saddle-point shapes.

[9] It proves convenient in the following to choose a unit normalization for the coefficients, e_i.

[10] Cf. Appendix I.

[11] Lowan, Davids, Levenson, Bull. Am. Math. Soc. **48**, 739 (1942).

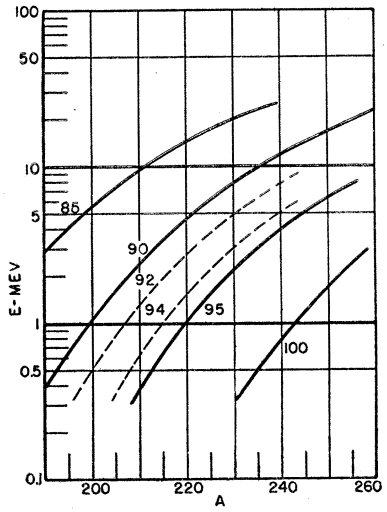

FIG. 3. Fission thresholds for nuclei near uranium. Curves for various Z values are given. Quantum-mechanical effects are not included.

integral of the singular part of $1/M$, the other the ith contribution to the numerical integral of the singular part. The details of this separation are given in Appendix II.

The change in the total energy of the nucleus produced by the deformation is expressed by the quantity

$$\xi \equiv \frac{\Delta E}{E_s^0} = B_s - 1 + 2x(B_c - 1). \qquad (23)$$

3. RESULTS

The most accurate and extensive study was made for $x=0.74$, the value calculated by Present, Knipp, and Reines[5] for U^{239}. The ξ-value found for its symmetric saddle-point is 0.013_6. (Cf. Table I.) This value coincides with the upper limit estimated by them;[12] the interpolated value given by Bohr and Wheeler[2] is 0.01_1.

The threshold value found for $x=0.90$, $\xi=0.0007$, agrees with the value found by Reines and Present. However at $x=0.81$, which bounds the range of validity of their series, their threshold value is some 8 percent less than the Eniac value, $\xi=0.0050$.

The threshold for $x=0.77$ was investigated briefly. An approximate threshold and saddle-point shape are given in Table I.

[12] We are indebted to Present, Reines, and Knipp for access to a more complete description of their work than their publication, reference 5.

The neighborhood of the saddle-point as determined by this procedure for $x=0.65$ was investigated with some care. The results obtained are listed in Table I.

The deformation shape near this indicated saddle-point ($x=0.65$) borders on the region in which multiple-valued R *vs.* μ description is required. The saddle-point shapes which have been obtained are shown in Fig. 1. It appears likely that for values of x somewhat less than 0.65 the true saddle-point shape requires a multiple-valued description and can therefore not be treated by the present method.

In Fig. 2a the values obtained for $(B_s-1)/(1-x)^2$ and $2(1-B_c)/(1-x)^2$ for the saddle-point shapes are plotted. Smooth curves have been drawn; the values at $x=1$ were taken from the series development of Bohr and Wheeler. In Fig. 2b the values obtained for $\xi/(1-x)^3$ are plotted. A smooth curve, consistent with the curves of Fig. 2a, is drawn: the initial value and slope are taken from Bohr and Wheeler. In Fig. 2c the maximum radii of the normalized saddle-point shapes are drawn.

In Fig. 3 the fission threshold (e.g., for photo-fission) is shown for nuclei near uranium. The constants used to evaluate these energies are those used by Present, Reines, and Knipp. They correspond to a value of 0.74 for x and to 538 Mev as the unit of energy in which ξ is measured for U^{239}. These energies may be regarded as the classical fission thresholds, i.e., the energy differences as computed with the liquid-drop model between the initial spherical equilibrium shape and the saddle-point unstable equilibrium shape.

Two quantum-mechanical effects must be taken into account in comparing observed photo-fission thresholds with the energies of Fig. 3. Photo-fission will be observed for energies below the saddle-point energy by reason of the tunnel effect. Moreover the zero-point energy of the mode of vibration which leads to fission effectively increases the energy of the equilibrium state. To calculate these effects requires the determination of a suitable trajectory of deformations leading to fission and of the momentum conjugate to the deformation coordinate so introduced.

To determine a suitable trajectory of deformations for a particular x value, say x_0, consider

first the quantum-mechanical problem of spontaneous fission which requires the traversal by tunnel effect of most of the region of positive ξ. The rate of spontaneous fission will be determined primarily by the minimum of the Gamow factor exponents for all such trajectories. It is clearly reasonable to suppose that a trajectory possessing this minimum value passes through or very close to the classical saddle-point of x_0. It furthermore seems reasonable to assume that this minimizing trajectory also lies close to the saddle-point deformations determined by other x-values than x_0. For this reason, and by reason of its convenience, the sequence of shapes of Fig. 1 is taken for the "fission trajectory." The maximum radius will be used as the coordinate specifying the deformation and will be denoted by $1+a$.

The evaluation of the Gamow factor requires the use of an effective mass, M_a, such that the kinetic energy associated with a motion along the fission trajectory is $\frac{1}{2}M_a(da/dt)^2$. Of all possible motions of an incompressible fluid consistent with the prescribed motion of the surface the minimum kinetic energy, hence, the minimum M_a is that of an irrotational motion. This minimum value of M_a is the value required for the Gamow factor calculation. The zero-rotation condition, together with the prescribed motion of the surface, uniquely determines the motion and permits the calculation of M_a.

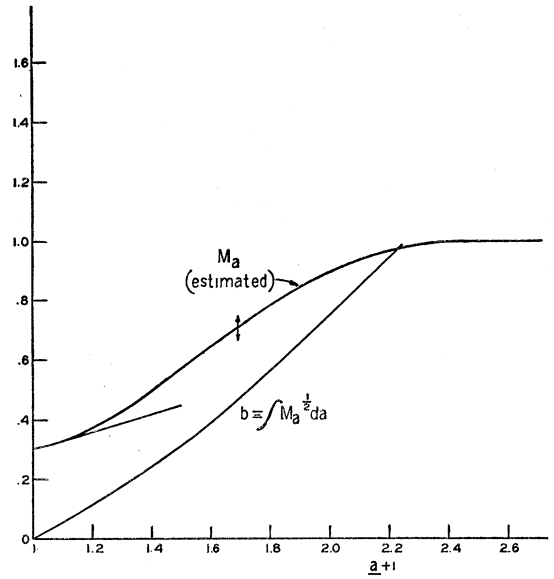

FIG. 4. The upper curve represents the effective mass for barrier penetration in units of the total mass. The lower curve is the transformed deformation coordinate b for which the effective mass is the total mass.

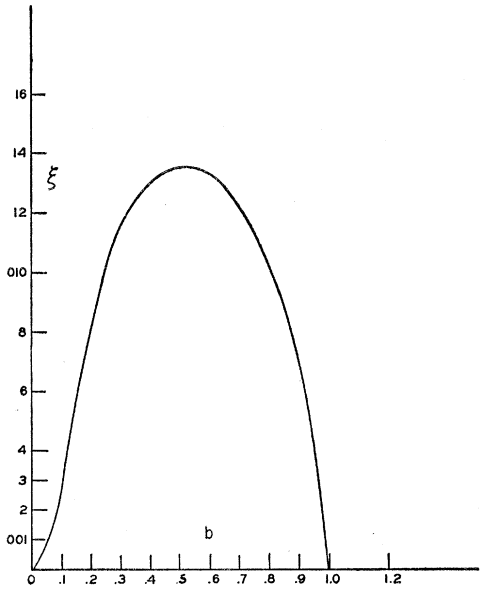

FIG. 5. The energy of deformation for $x=0.74$. The coordinate b is plotted in Fig. 4. The unit of energy is taken as 538 Mev and the unit of length is the initial nuclear radius.

For small a the surface is described by

$$R(\mu)=1+aP_2(\mu)+0(a^2).$$

The pattern of motion can be shown to be

$$\bar{v}=(da/dt)\ \mathrm{grad}(r^2P_2(\mu))$$

and

$$M_a=0.3M(1+a)+0(a^2),$$

where M is the total mass of the nucleus. After fission (i.e., for large a) M_a approaches M. A numerical calculation has been carried out for one intermediate value of a, $a=0.69$ corresponding to the saddle-point for $x=0.74$. The value obtained is $M_a=0.71M$ with an estimated probable error of 5 percent. These values were used to draw the approximate M_a *vs.* a curve of Fig. 4. This determination of M_a permits the transformation to another coordinate specifying the deformation,

$$b=\int(M_a/M)^{\frac{1}{2}}da,$$

for which the effective mass is the total mass, M.

In Fig. 5 the energy of deformation is drawn as a function of this deformation coordinate, b, for $x=0.74$. The unit of energy is E_s^0 which for values of the mass number, A, near 238 is taken to be 538 Mev as determined by Feenberg.[13] The unit of length in which b is measured is the initial nuclear radius which is taken as $A^{\frac{1}{3}}1.47\times10^{-13}$ cm as determined by Bohr and Wheeler.[2]

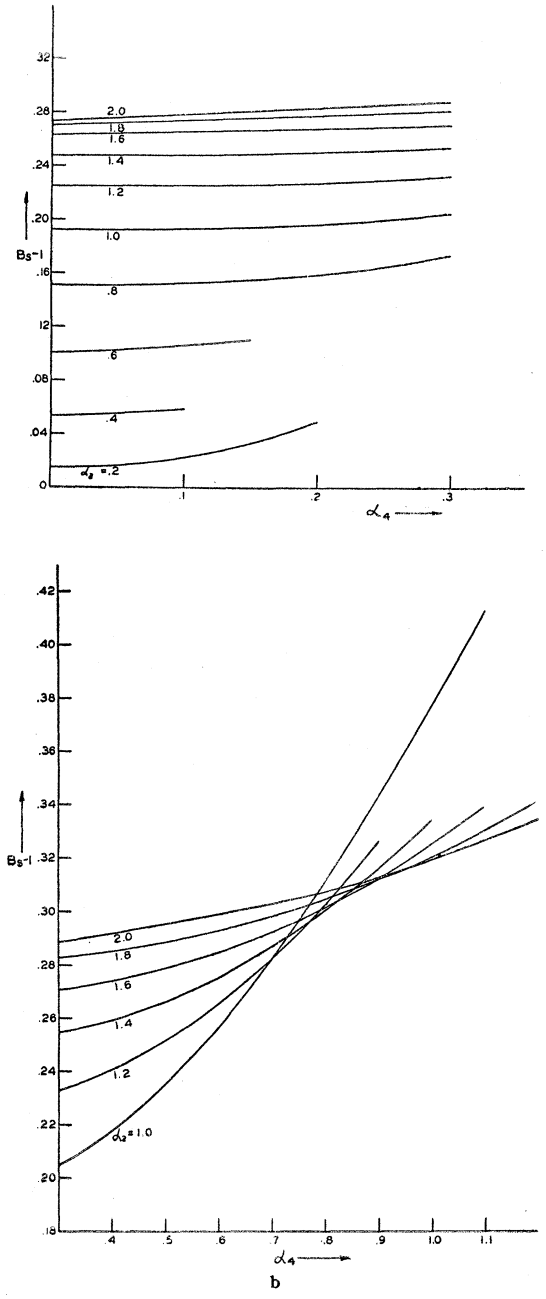

FIG. 6. Relative surface energies as functions of the deformation parameters α_2, α_4; cf. Eq. (3).

[13] E. Feenberg, Phys. Rev. **55**, 504 (1939).

The energy *vs.* deformation relationship of Fig. 5 has been used to calculate the Gamow penetration probability for various excitation energies. This penetration probability is found to be well represented by

$$G=10^{-7.85\Delta E}, \tag{24}$$

where ΔE is the energy deficit at the saddle-point in Mev.

The zero-point energy of vibration as calculated with the initial curvature of Fig. 5 is 0.4 Mev corresponding to a vibration frequency of 2×10^{20} sec.$^{-1}$ in agreement with the value calculated by Bohr and Wheeler.[2]

Using this value for the zero-point energy and Eq. (24), the mean life for spontaneous fission may be calculated.[14]

$$T_s=10^{-21}\ \text{sec}/G=10^{26}\ \text{yr}. \tag{25}$$

(Cf. Table II.)

The excitation energy required for fission will be approximately E_{cl} less the zero-point energy, 0.4 Mev., where

$$E_{cl}=E_s^0\xi_{\max}.$$

A corresponding set of values has been calculated for $x=0.75$. The results are listed in Table II. It will be seen there that if x is assumed to have the value 0.74 for U^{238}, reasonable agreement with experimental results on photo-fission[15] and spontaneous fission[16] is obtained. This choice represents a slight revision of the conclusions reached by Bohr and Wheeler who chose $x=0.74$ by similar considerations based on their interpolated ξ-curve.

It should be noted that the fission trajectories for which these calculations have been made are not precise minimal trajectories, thus the mean-life values for spontaneous fission given in Table II are upper limits.

[14] T_s is reduced by a factor of 5 for the degeneracy of this mode of vibration. Cf. reference 2.

[15] R. O. Haxby, W. E. Shoupp, W. E. Stephens, and W. H. Wells, Phys. Rev. **59**, 57 (1941).

[16] G. Scharff-Goldhaber and G. S. Klaiber, Phys. Rev. **70**, 229 (1946); W. Maurer and H. Pose, Zeits. f. Physik **121**, 285 (1943); H. Pose, Zeits. f. Physik **121**, 293 (1943); G. N. Flerov and K. A. Petrzhak, J. Phys. U.S.S.R. **3**, 275 (1940).

In order to represent deformation energies for shapes other than those on the assumed fission trajectories, a number of Eniac calculations were performed for deformations specified by various values of α_2 and α_4, with all other α's vanishing. The values obtained for B_s and B_c are presented separately in Figs. 6a, 6b and 7a, 7b. The corresponding ξ-values for $x=0.74$ are shown in Fig. 8. It may be noted (cf. Fig. 1) that the saddle-points for $x \geqslant 0.74$ are closely approximated in this α_2, α_4 representation.

4. ASYMMETRIC DEFORMATIONS

Deformation energies, B_s, B_c, and ξ have been calculated for a few asymmetric shapes. Unfortunately this investigation was by no means complete or systematic.

It is to be expected that the interesting effects due to asymmetric terms in the $R(\alpha)$ expansion, Eq. (3), will arise primarily from the P_1 and P_3 terms. The higher odd harmonics will serve primarily as refinements as do the higher even harmonics in symmetric fission. The use of odd harmonics introduces one "spurious" degree of freedom since a symmetric deformation shape can be represented by an asymmetric series if the origin of the polar-coordinate systen is displaced along the axis of (rotational) symmetry. This degeneracy of the description may be removed by the imposition of one condition on the expansion coefficients. A convenient form for this condition is the requirement that the center of gravity shall remain at the origin. In the present work no such condition was systematically applied. The effect of the addition of various combinations of P_1 and P_3 to a few symmetric expansions was determined.

It was hoped that this brief investigation of asymmetric shapes might lead to an explanation of the observed asymmetry of fission.[17] However no evidence was found that the influences producing the asymmetry of fission are represented in this model.

Small amounts of P_1 and P_3 were added to the initial spherical shape. The B_s and B_c values obtained were consistent with the power series expansion of Bohr and Wheeler (reference 2, Eq. (9)).

$$B_s=1+5\alpha_3^2/7+0(\alpha^4),$$
$$B_c=1-10\alpha_3^2/49+0(\alpha^4). \qquad (26)$$

In these expansions there are no terms in α_1^2 because to this order the introduction of a P_1 component serves merely to displace the drop

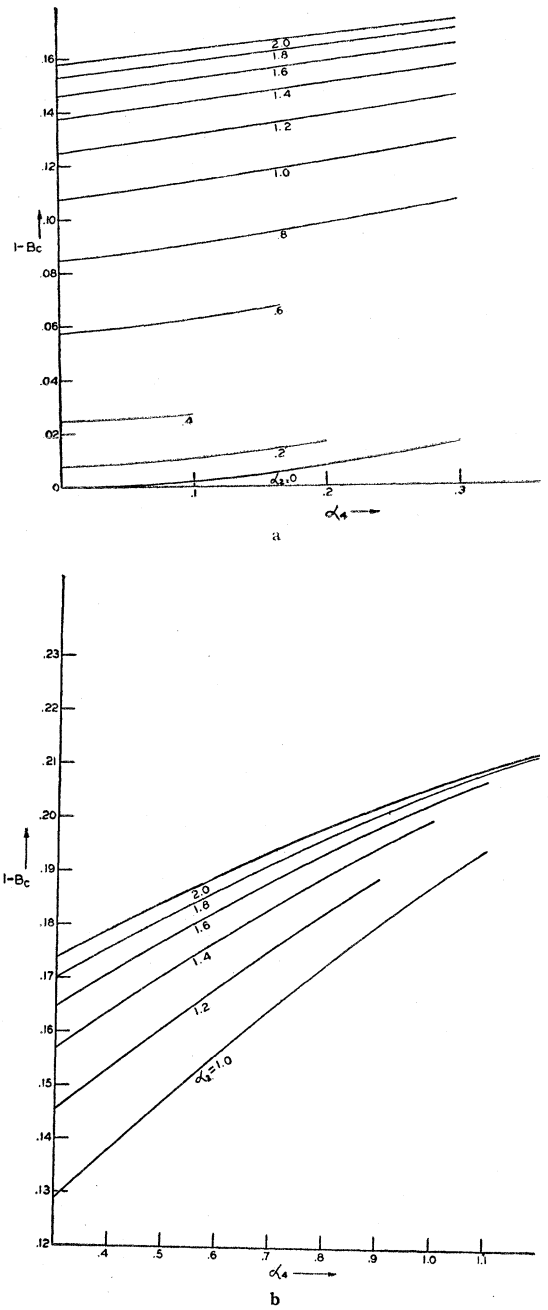

FIG. 7. Relative Coulomb energies as functions of α_2, α_4.

[17] The Plutonium Project, Rev. Mod. Phys. 18, 513 (1946).

TABLE II. Energies and mean lives for $E_s^0=538$ Mev., $A=238$, $r_0=1.47\times10^{-13}$.

x	ξ	$E_{ci}-0.4$ (Mev.)	T_s (yrs.)
0.74	0.0137	6.9_7	10^{26}
0.75	0.0120	6.0_7	10^{17}

parallel to the polar axis. Thus for small deformations from the spherical shape the center of gravity condition is approximately equivalent to the restriction $\alpha_1=0$.

More generally, a small displacement, δ, parallel to the polar axis, transforms the expansion

$$R(\mu)=1+\sum\alpha_iP_i(\mu)$$

to

$$R'(\mu)=1+\sum\alpha_iP_i+P_1\delta+(\delta/R)\sum\alpha_i\frac{i(i+1)}{2i+1}(P_{i+1}-P_{i-1})+0(\delta^2). \quad (27)$$

Thus for the sphere, $R(\mu)=1$, the displacement is described by a change in α_1 alone. However, for a shape such as

$$R=1+0.7P_2$$

(an approximate saddle-point for $x=0.74$) which becomes

$$R'=1+0.7P_2+P_1\delta+[0.84\delta/(1+0.7P_2)]\times(P_3-P_1)+0(\delta^2)$$
$$=1+0.7P_2+0.20\delta P_1+1.05\delta P_3-0.28\delta P_5+\cdots,$$

the principal effect of the displacement is to change α_3. Thus in the neighborhood of the heavy-nucleus thresholds the effect of α_3 is of secondary interest while α_1 makes the important contribution to the asymmetry. For the deformation shape

$$R=(1+0.7P_2)+\alpha_1P_1,$$
$$\xi=(1.12783-0.247\alpha_1^2)+2x(-0.07132+0.238\alpha_1^2)+0(\alpha_1^4). \quad (28)$$

Thus for $x>0.52$ the deformation energy is *increased* by this introduction of asymmetry. It should be noted that the effect on the deformation shape of the term α_1P_1 is to narrow the "neck," i.e., the relative minimum of $R(1-\mu^2)^{\frac{1}{2}}$, in comparison with the length. Thus in addition to the introduction of asymmetry, this term has a geometric effect similar to that of an increase of α_2. On the other hand the introduction of asymmetry, by shiting material from one side to the other, has in part the effect of restoring the original spherical shape. Thus the P_1 term has two effects, that of producing asymmetry and that of changing the symmetric distortion in an ambiguous way. As α_2 is increased from 0.7, ξ increases if $x<0.88$, decreases if $x>0.88$ (cf. Figs. 6–7). Since the P_1 term increases ξ throughout the range $0.52<x<1.00$ it seems likely that that part of its effect due only to asymmetry is uniformly unfavorable.

For a more quantitative study of the effect of asymmetry on the deformation energy, small amounts of P_1 and P_3 were added to the symmetric saddle-point expansion for $x=0.77$. It may be seen from Eq. (27) that the displacement by a distance δ of a symmetric-deformation shape introduces changes in the even-harmonic coefficients, α_2, α_4, etc., of order δ^2. At the saddle-point these changes affect the deformation energy only to order δ^4. Thus if small odd-harmonic terms are added to the saddle-point expansion the change in ξ of order α_{odd}^2 is due entirely to the true asymmetry which they produce and not the change in the symmetric distortion produced by their "equivalent displacement." The change in ξ for small α_{odd} was found to be

$$\Delta\xi_{x=0.77}\cong0.246(0.659\alpha_1-0.752\alpha_3)^2+0.010(0.752\alpha_1+0.659\alpha_3)^2. \quad (29)$$

The coefficient of the second term would be zero if all the odd terms produced by a displacement were taken into account. The corresponding expression for the (spherical) saddle-point of $x=1.0$ is (cf. Eq. (26))

$$\Delta\xi_{x=1.0}=0.306\alpha_3^2+0.000\alpha_1^2. \quad (30)$$

The slight decrease in the first coefficient as x decreases from 1.0 to 0.77 suggests that with increasing symmetric deformation a small amount of asymmetry becomes energetically less unfavorable and may even become favorable for very great distortion. To check this possibility the deformation energy has been calculated analytically for the extreme deformation represented by two spheres in contact.[18] The

[18] We are indebted to Dr. John Mauchly and to Dr. Leonard Schiff for this suggestion.

result is

$$\xi=(V^{\frac{2}{3}}+W^{\frac{2}{3}})-1+2x[V^{5/3}+W^{5/3}+5VW/3(V^{\frac{1}{3}}+W^{\frac{1}{3}})-1], \quad (31)$$

where V and W are the fractions of the original volume in the two spheres. The derivative,

$$d\xi/dV=2(V^{\frac{1}{3}}-W^{\frac{1}{3}})/3V^{\frac{1}{3}}W^{\frac{1}{3}}\times[20xV^{\frac{2}{3}}W^{\frac{2}{3}}/3(V^{\frac{1}{3}}+W^{\frac{1}{3}})-1]$$

consists of two factors, the first increasing from 0 to $+\infty$ as V increases from 0.5 to 1.0, the second decreasing monotonically from $5x/3-1$ to -1. Thus for $x>0.6$, ξ has a relative minimum at $V=W=0.5$ and no other. For $x<0.6$ no minimum exists. Figure 9 shows the dependence of ξ on V for various x-values.

In order to compare this result with the previously evaluated effects of asymmetry, Eqs. (29) and (30), the two-sphere shape may be expressed in a form analogous to the Legendre polynomial expansion.

$$R=2|\mu|+\alpha_1\mu=(1+\alpha_2P_2+\alpha_4P_4+\cdots)+\alpha_1P_1$$

where

$$\alpha_{2n}=\tfrac{1}{2}(4n+1)\int_{-1}^{1}P_{2n}(\mu)2|\mu|d\mu.$$

Reexpressing the energy, Eq. (31), by the use of the relationship

$$V=(1+\alpha_1/2)^3/2(1+3\alpha_1^2/4)$$

gives

$$\Delta\xi=2^{1/3}(1+17x/12)+2^{-5/3}(5x/3-1)\alpha_1^2+\cdots.$$

For $x=0.75$ (for example) the coefficient of α_1^2 is 0.0788, which is considerably smaller than the leading coefficients in Eqs. (29) and (30) but is still appreciably greater than zero. Figure 9 shows, moreover, that the increase of energy with increasing asymmetry extends to quite great asymmetries.

The above evidence seems to us to suggest strongly, although not to prove conclusively, that asymmetric fission is not favored in the liquid-drop model.

ACKNOWLEDGMENTS

We wish to thank the Army Ordnance Department and the University of Pennsylvania, particularly General G. M. Barnes, Colonel L. E. Simon, and Dr. L. S. Dederick for the use of the Eniac and to Professor J. von Neumann and Dr. and Mrs. H. H. Goldstine for instruction in its operation. We particularly wish to acknowledge our indebtedness to the capable operating staff of the Eniac, who proved quite indispensable in

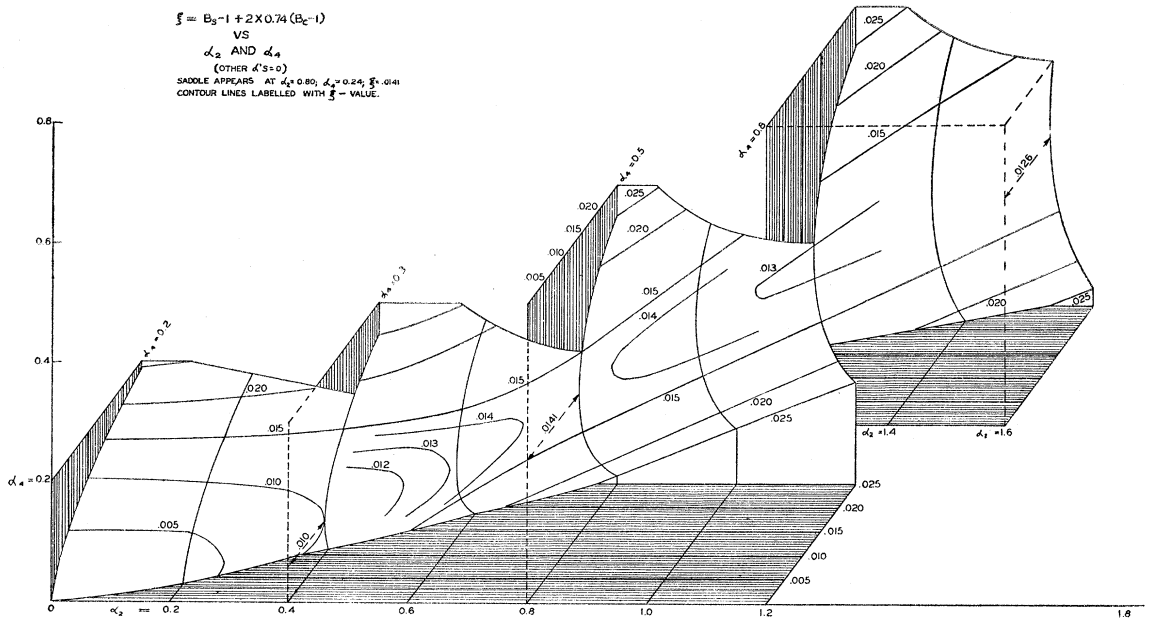

FIG. 8. Relative total energies as functions of α_2, α_4 for $x=0.74$.

the execution of this and a preceding problem. We are also indebted to Professors E. Fermi and E. Teller, Mr. J. P. Eckert, Jr., and Dr. J. Mauchly for their help in many valuable discussions.

APPENDIX I

An Alternative Radial Integration Rule

An alternative integration rule (analogous to the Gauss rules) was developed for use in the event that the rule of Eq. (15) proved insufficiently accurate. The gauss rules for the approximate evaluation of integrals in the range $(-1, 1)$ with unit weight factor are based on the orthogonality property of the legendre polynomials in this range and with this weight. For the present problem we make use of the polynomial, $F_4(x)$, which is orthogonal to polynomials of lower degree with the weight factor x^2.

This polynomial can be constructed from the legendre polynomials, P_i, scaled to the interval (0,1),

$$p_i(x) \equiv P_i(2x-1),$$

$$x^2F_4(x) = \begin{vmatrix} p_4(x) & p_5(x) & p_6(x) \\ p_4(0) & p_5(0) & p_6(0) \\ p_4'(0) & p_5'(0) & p_6'(0) \end{vmatrix}.$$

The determinant and its first derivative evidently vanish at $x=0$, thus it does contain the factor x^2. $x^2F_4(x)$ is a linear combination of $p_4(x)$, $p_5(x)$, and $p_6(x)$ and is therefore orthogonal to any cubic polynomial in (0,1). Any seventh degree polynomial, $f_7(x)$ may be divided by $F_4(x)$ leaving a cubic remainder.

$$f_7(x) = Q_3(x)F_4(x) + R_3(x)$$

thus

$$\int_0^1 f_7(x)x^2dx = \int_0^1 R_3(x)x^2dx.$$

If x_j is one of the four (real) roots of $F_4(x)$

$$f_7(x_j) = R_3(x_j).$$

The cubic polynomial, $R_3(x)$, may be expressed in terms of these four of its values

$$R_3(x) = \sum_{j=1}^{4} R_3(x_j)F_4(x)/(x-x_j)F_4'(x_j),$$

thus

$$3\int_0^1 f_7(x)x^2dx = \sum_{j=1}^{4} e_j f_7(x_j)$$

where

$$e_j = 3\int_0^1 [x^2F_4(x)/(x-x_j)F_4'(x_j)]dx.$$

The roots and coefficients have the values

$$x_j = 0.204149,\ 0.482953,\ 0.761399,\ 0.951499,$$
$$e_j = 0.031057,\ 0.205902,\ 0.430376,\ 0.332665.$$

This method can obviously be extended to other weight functions and to other numbers of entries.

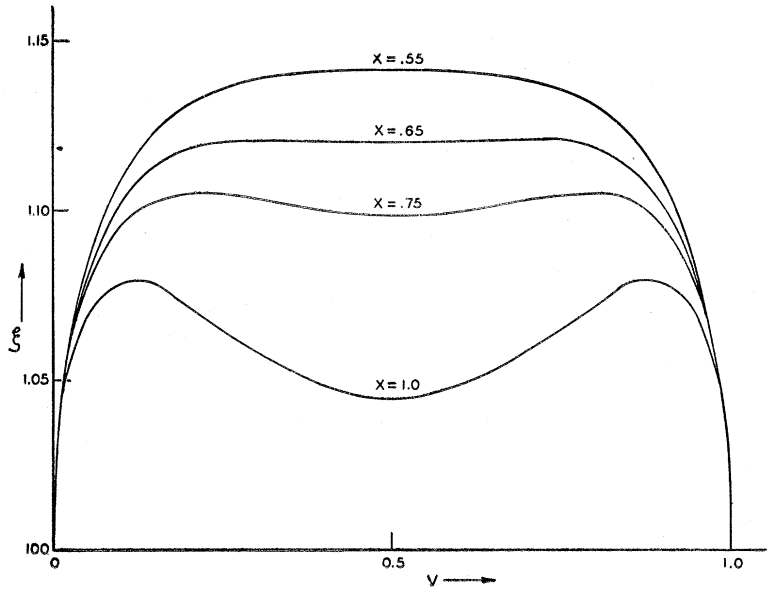

FIG. 9. The energy of deformation corresponding to two spheres in contact as a function of the fractional volume V for various x values. No central minimum exists for $x<0.60$.

APPENDIX II

The separation of the singular part of the surface integral.

The integral

$$B_c = V^{-5/3}\int_{-1}^{1}\tfrac{1}{2}d\mu\int_{-1}^{1}\tfrac{1}{2}d\mu'\int_{0}^{1}3x^2dx \times R^3(\mu)R^3(\mu')/M(\mu,\mu',x)$$

is to be approximated by the finite sum of Eq. (20). Special treatment is required for $x=1.0$ ($k=5$ in Eq. (20)) since there the μ' integral is singular. For small values of $|\mu-\mu'|$, $1/M(\mu,\mu',1)$ becomes infinite as $-\ln|\mu-\mu'|/R$. Thus the integral over μ' may be separated as

$$\int[R'^3/M(\mu,\mu',1)]\tfrac{1}{2}d\mu' = \int[R'^3/M+R^2(\mu)\ln|\mu-\mu'|/\pi]\tfrac{1}{2}d\mu' + R^2(\mu)\psi(\mu)/\pi, \quad (32)$$

where

$$\psi(\mu) = -\int_{-1}^{1}\tfrac{1}{2}d\mu'\ln|\mu-\mu'| = 1-\tfrac{1}{2}\ln(1-\mu^2)-\tfrac{1}{2}\mu\ln\frac{1+\mu}{1-\mu}.$$

The remaining integrand is now sufficiently smooth to permit numerical integration. Its value for $\mu=\mu'$ is, apart from the factor R'^3,

$$\frac{1}{2\pi R}\ln\left[\frac{64R^2(1-\mu^2)}{R^2+(1-\mu^2)(dR/d\mu)^2}\right]. \quad (33)$$

To evaluate this quantity the minimum distance, A_0 of Eqs. (11) and (12), is given (instead of zero) the value

$$\epsilon=\delta[(dR/d\mu)^2+R^2/(1-\mu^2)]^{\frac{1}{2}}, \quad 0<\delta\ll 1, \quad \mu=\mu_i, \quad R=R(\mu_i)$$

and the iterative process carried out to determine $1/M_i$. The expression (33) then has the value

$$1/M_i+Q/R$$

where

$$Q=\ln\delta/\pi+0(\delta^2\ln\delta).$$

Now approximating the integral of the right side of Eq. (32) by the gaussian integration formula gives

$$\int[R'^3/M(\mu_i,\mu',1)]\tfrac{1}{2}d\mu' \cong R_i^2\psi(\mu_i)/\pi + \sum_{j\neq i}c_j[R_j^3/M_{ij5}+R_i^2\ln|\mu_i-\mu_3|/\pi] + c_iR_i^3[1/M_i+Q/R_i]=\sum_{j=1}^{10}c_jR_j^3\lambda_{ij}, \quad (34)$$

where

$$\lambda_{ij}=1/M_{ij5} \quad \text{for } j\neq i$$
$$=1/M_i+P_i/R_i \quad \text{for } j=i$$
$$P_i=\psi(\mu_i)/\pi c_i+\sum_{j\neq 1}c_j\ln|\mu_i-\mu_j|/\pi c_i+Q.$$

In calculating ϵ, δ was taken as 10^{-4}. The remaining factor in ϵ is the ratio of two numbers available at this stage of the calculation. The ten constants, P_i, were stored in a function table. In the Eniac routine it was possible to make the above indicated changes in procedure at the "singular points" with relative ease: the numbers entering into the calculation of $1/M$ were there chosen in a special way. Because of the smallness of δ the number of iterations (Eq. 12) was doubled. $1/M$ is added to P_i/R_i and is then entered into the series in the normal fashion.